2008 IEEE International Conference on
Robotics and Automation
Pasadena, CA, USA, May 19-23, 2008

Experimental Validation of a Fuel-Efficient Robotic Maneuver Control Algorithm for Very Large Flexible Space Structures

Masahiro Ono, Peggy Boning, Tatsuro Nohara, and Steven Dubowsky

***Abstract*—The robotic maneuvering of large space structures is key to a number of future orbital missions. In this paper a large space structure maneuver control algorithm, recently proposed, is extended and experimentally validated. The method uses space robots' manipulators to control the vibration of the structures being maneuvered and their reaction jets perform the large motion maneuvers. The algorithm quickly damps out the vibrations and requires less fuel than reaction jet-based vibration control methods. The approach is called *maneuver decoupled control.* Its performance is demonstrated and quantitatively evaluated in simulation and experiments.**

I. Introduction

SPACE robotics is one of the key technologies for the future on-orbit construction of large space structures as for large orbital telescopes, space solar power plants and space stations [8,12] (see Fig. 1). For some applications these structures will have dimensions in the 1000's of meters [11]. The assembly of the International Space Station has shown that human construction in space is very expensive, slow, and dangerous. Studies suggest that robotic on-orbit operation would be faster, safer and much less expensive [17].

When maneuvering large space structures, vibration control is an important problem since the structures are thin and flexible to minimize launch cost. The natural damping of such flexible space structures in space is very small. Space construction robots will need to actively control the vibration of these structures, while maneuvering them, to prevent delays in the construction, or damage of the structures and/or the robots.

There has been a significant amount of work in the area of controlling flexible space structures and spacecraft [1][2][3][4][6][14][16]. An on-orbit vibration control experiment was conducted using the Japanese satellite ETS-VI [10]. Most of these works have focused on the vibration control of the flexible structures firmly attached to the spacecraft such as solar arrays and antennas.

These on-orbit vibration control methods are not suitable for the future construction of very large space structure for two reasons. First, in these algorithms the flexible elements are assumed to be an integral part of the spacecraft with their actuators and sensors. In the future construction of very large space structure will require the assembly of many large passive structural subassemblies that will be manipulated by other spacecraft (i.e. space robots). It would not be practical to provide thrusters, reaction wheels, or piezoelectric actuators in the subassemblies. Second, as these large space structures will require the assembly of hundreds of subassemblies, controlling their vibration by reaction jet is not practical. Reaction jet fuel is a very expensive resource on-orbit.

A new vibration control algorithm for space structure maneuvering has been recently proposed [9]. In this approach the robots' manipulators are used to control the vibration of flexible structures. The reaction jets only control the gross motion of the system. The control, called *maneuver decoupled control*, separates the coupled dynamics of the robot and the flexible structure system. It has been shown to be effective in simulations. In this work, the flexible structure is modeled as a passive object held by space robots. Its manipulators are used to control the vibration. These manipulators can be powered with only limited restriction from photo-voltaic solar arrays. This approach is shown to substantially reduce reaction jet fuel consumption and reduce the plume impingement problem [15][18].

It has been found that this control was sensitive to sensor noise and actuation errors [13]. Here the decoupled controller is extended to provide robustness to noise and to actuation errors. The effectiveness of this extended controller is experimentally validated. The experiments were performed on *The MIT Field and Space Robotics Lab (FSRL) Free-Flying Robotics Test Bed (FFRT)* (see Fig. 2).

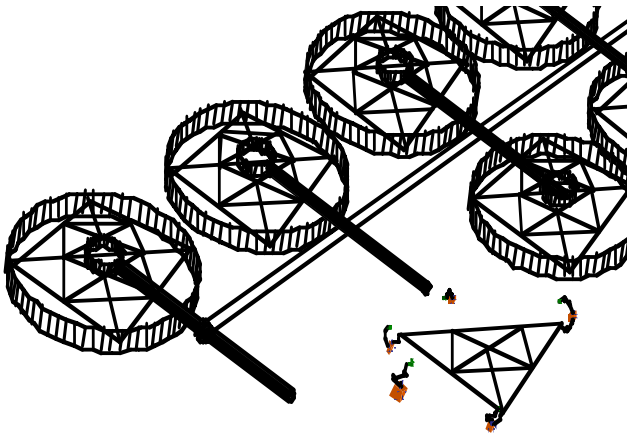

Fig. 1. A concept for on-orbit robotic construction of flexible structures

This work was supported by Japan Aerospace Exploration Agency.

The authors are from the Field and Space Robotics Laboratory in the Mechanical Engineering Department at the Massachusetts Institute of Technology, 77 Massachusetts Avenue, MA, USA (corresponding email: pboning@mit.edu).

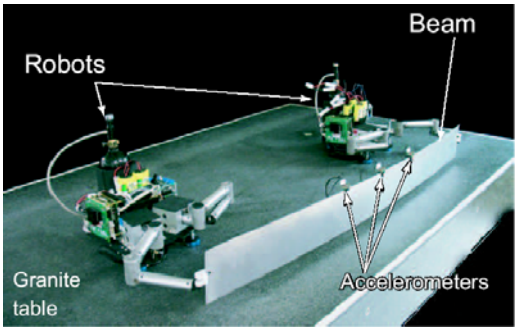

Fig. 2. The MIT FSRL Free-Flying Robotics Test Bed (FFRT)

II. Analytical Development

The decoupled controller proposed by Y. Ishijima is modified and used to control the coupled dynamics of the structure and the robots [9]. A simple control problem is show in Fig. 3 where two robots are cooperatively maneuvering a flexible structure. The original decoupled controller consists of a vibration controller and a rigid-body controller. The vibration controller is a LQR state feedback controller using robots' manipulators that control the structural element's vibration. It uses the estimated states of vibration of the structural element as the input, and provides force commands to the manipulators. The rigid-body controller is a classical PD controller. It uses the robot's position and velocity to determine the required thruster force.

The original decoupled controller is modified by including a manipulator compliance controller between the robot and the structural elements. This controller bridges the above controllers and was found experimentally to make the system more robust to assembly errors and noise. Hence, the decoupled controller used in this work consists of three controllers: the vibration controller, the rigid-body motion controller, and the manipulator compliance controller.

A. Vibration Controller

This controller is a LQG state feedback controller:

$$\begin{bmatrix} F_{mp,y1} \\ F_{mp,y2} \end{bmatrix} = K_{lqr} \begin{bmatrix} \hat{q} \\ \hat{\dot{q}} \\ \hat{F}_{mp,y1} \\ \hat{F}_{mp,y2} \end{bmatrix} \qquad (1)$$

where $\hat{q}$ are the estimated modal coordinates and $\hat{\dot{q}}$ are their derivatives, $F_{mp,\,yi}$ is the component of the force applied to the structural element in the direction of bending by the ith robot's manipulator, and $\hat{F}_{mp,yi}$ is the measured manipulator force and contains measurement error and noise. A Kalman filter is used to obtain $\hat{q}$ and $\hat{\dot{q}}$.

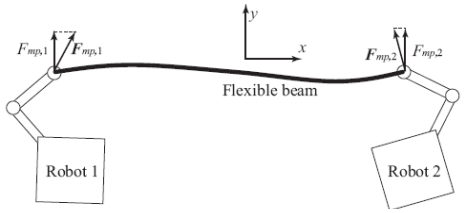

Fig. 3. Robots maneuvering a flexible structure

To find the optimal LQR gain K_{lqr}, the following linearized dynamics model of structural elements is used. This model neglects rotational and Coriolis effects. Delays due to the low-level controllers and actuators of the robots are included in the model.

$$\dot{x} = Ax + Bu \qquad (2)$$

$$x = \begin{bmatrix} q \\ \dot{q} \\ F_{mp,y1} \\ F_{mp,y2} \end{bmatrix} \qquad (3)$$

$$u = \begin{bmatrix} F_{mp,y1,des} \\ F_{mp,y2,des} \end{bmatrix} \qquad (4)$$

$$A = \begin{bmatrix} 0 & 1 & 0 & 0 \\ -\Omega^2 & -2Z\Omega & M^{-1}\Phi_1 & M^{-1}\Phi_2 \\ 0 & 0 & -1/\tau & 0 \\ 0 & 0 & 0 & -1/\tau \end{bmatrix} \qquad (5)$$

$$B = \begin{bmatrix} 0 & 0 \\ 0 & 0 \\ 1/\tau & 0 \\ 0 & 1/\tau \end{bmatrix} \qquad (6)$$

where τ is the time constant of the delay and $F_{mp,yi}$ is the actual manipulator force while $F_{mp,yi,des,}$ is the desired (commanded) manipulator force. The matrices Z and Ω are diagonal and their elements are damping ratios and natural frequencies of corresponding vibration modes respectively. The constant Φ_i is the normalized amplitude of the mode shape at the point where the ith robot holds the structural element. The matrix M is the diagonal modal mass matrix. For a beam-like structure, the nth diagonal elements of M are defined as follows using mode shape Φ_n:

$$M_n = m\int_{y=0}^{y=L} \Phi_n(y)\cdot\Phi_n(y)dy \qquad (7)$$

where the y-axis runs along the beam's length.

Using this model, the state feedback gain K_{lqr} is obtained by solving infinite horizon Riccati equation so that the following performance metric J is minimized:

$$J = \int_0^\infty (x^T Qx + u^T Ru)dt \qquad (8)$$

where the matrices Q and R determine the relative weighting of state error to controller effort. Note that the state vector x does not include the rigid-body modes of the system. Therefore the vibration controller does not control the rigid-body motion of the structural element.

B. Rigid-Body Motion Controller

The rigid-body position and velocity of the system are controlled by thrusters. While many algorithms could be use, here simple PD control is employed. The thruster force is given by:

$$F_{th} = K_{p,th}(x_c - x_{robot}) + K_{d,th}(\dot{x}_c - \dot{x}_{robot}) \qquad (9)$$

where x_c and $\dot{x}_c$ are desired position and velocity, and x_{robot} and $\dot{x}_{robot}$ are measured position and velocity. $K_{p,th}$ and $K_{d,th}$ are the proportional and differential gain.

C. Manipulator Compliance Controller

The manipulator compliance controller is also a simple PD controller which behaves like a spring and a damper between the manipulator's end effector and a reference point, fixed in the robot's local coordinate system:

$$F_{th} = K_{p,acc}(r_{EE} - r_{ref}) + K_{d,acc}(\dot{r}_{EE} - \dot{r}_{ref}) \qquad (10)$$

where r_{EE} is the end effector position, r_{ref} is the position of the reference point, $K_{p,acc}$ and $K_{d,acc}$ are the proportional and differential gains [7]. Note that Eq. (10) is described in the robot's local coordinates fixed to the robot's body. This controller ties the vibration controller (Section II-A) and the rigid-body controller (Section II-B). The entire controller design is shown in the block diagram in Fig. 4.

III. Predicted Simulation Results

To quantitatively evaluate the proposed controller's performance, the following three methods were considered:

No vibration control: Two robots simply transport a beam using thrusters without controlling the vibration. The joints of the robot manipulators are locked.

Thruster vibration control: The robots both transport a beam and control its vibration using their thrusters. Again, the joints of the manipulators are locked.

Maneuver Decoupled Control: The robots transport a beam using their thrusters while controlling the vibration using their manipulators.

These control methods were studied in simulation. The simulation model includes actuator and sensor errors. Fig. 5 compares the magnitude of vibrations with three control methods: no vibration control, thruster vibration control, and vibration control with manipulators (the maneuver decoupled controller). From the figure it is obvious that the decoupled controller damps the vibration most quickly. There is not a visible difference between the performances of the two other controllers.

This is because the thruster has very small thrust (0.1N), and robots are large compared to the beam mass. A relatively large spike is observed at the beginning of the simulation in the decoupled controller. This is because the vibration state estimator (Kalman filter) had an initial error and the decoupled controller calculated the manipulator force based on imprecise information. After the estimator converged (t ≈ 0.5 seconds), the controller successfully controlled the vibration.

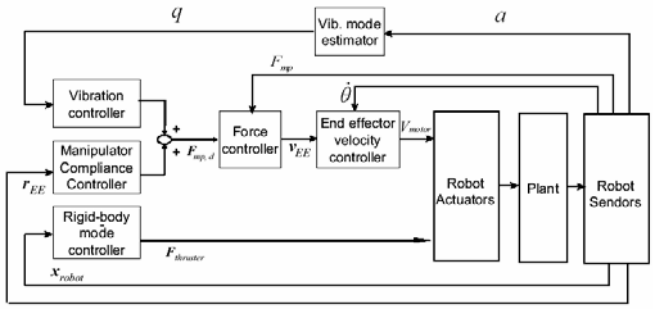

Fig. 4. Controller block diagram.

Fig. 6 shows accumulated fuel consumption versus time. A large part of the fuel consumption is used for base motion. Fig. 7 summarizes the result. In both cases, decoupled control with the manipulators achieves a higher damping ratio while consuming less fuel when compared to thruster vibration control. For the rotational maneuver, the fuel consumption of decoupled control is even less than no vibration control. When the beam vibrates, the robots' position also vibrates due to the coupled dynamics. The robots consume extra fuel to control this disturbance to the robots even with no active vibration control.

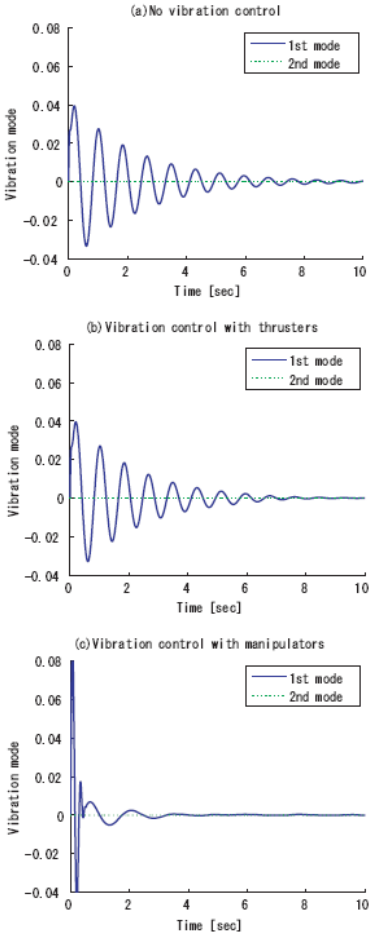

Fig. 5. The simulated first mode vibration. Top: (a) No vibration control. Middle: (b) Thruster vibration control. Bottom: (c) Decoupled control (Vibration control by manipulators)

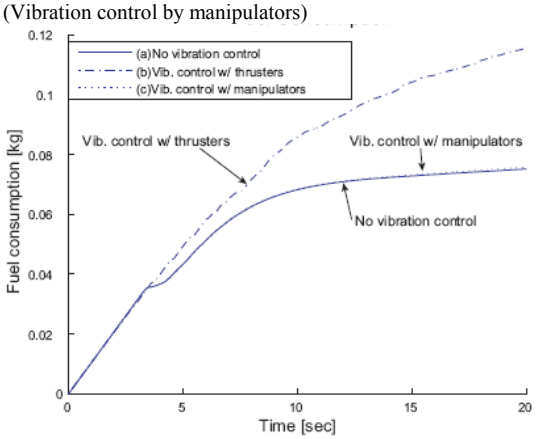

Fig. 6. Fuel consumption by control method (simulation result)

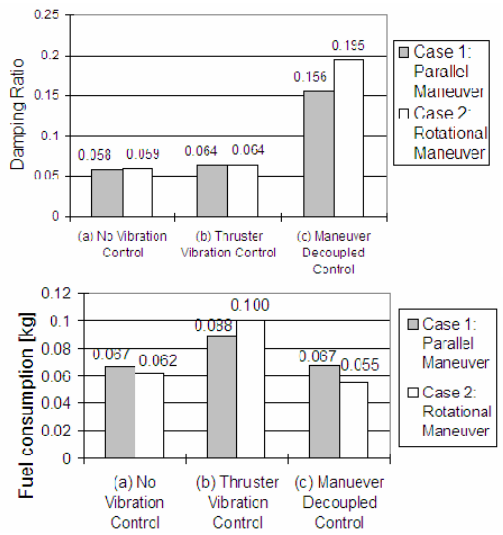

Fig. 7. Damping ratio and fuel consumption of three control methods for parallel and rotational maneuvers (simulation results)

IV. Experimental Validation

While the above simulation results show the potential of this approach experimental validation is essential. These experiments were performed using the MIT Field and Space Robotics Lab (FSRL) Free-Flying Robotics Test Bed (FFRT), see Fig. 2.

The FFRT consists of a number of kilogram scale multi-arm manipulator robots floating on CO_2 bearings to emulate microgravity in two dimensions [5]. It uses a 1.3 m x 2.2 m granite table for small scale experiments and a large polished epoxy floor (4.8 m dia) at the MIT Space Systems Laboratory (SSL) for larger scale experiments (see Fig. 8). The robots are equipped with two manipulators, eight thrusters, two position sensors, four manipulator joint angle encoders, and two force/torque sensors (see Fig. 9). The robots have 7 DOF in total (2 DOF translation, 1 DOF rotation, and 4 DOF manipulator joints), all of which are controllable and observable. All actuators and sensors are controlled by the on-board computer and powered by on-board batteries, so that the robots can work without any externally connected cables. The robots have Wireless LAN adapters to give an experiment operator access to the on-board computer. Each robot weighs approximately 7 kg. The maximum thruster force is approximately 0.1 N. The robots float on the flat table using CO_2 air bearings, emulating weightlessness in the two-dimensional plane.

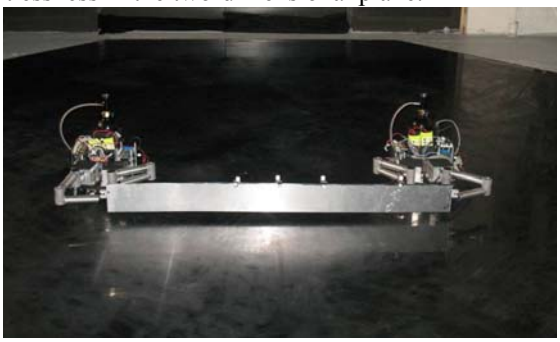

Fig. 8. The MIT Space Systems Laboratory (SSL) Flat Epoxy Floor

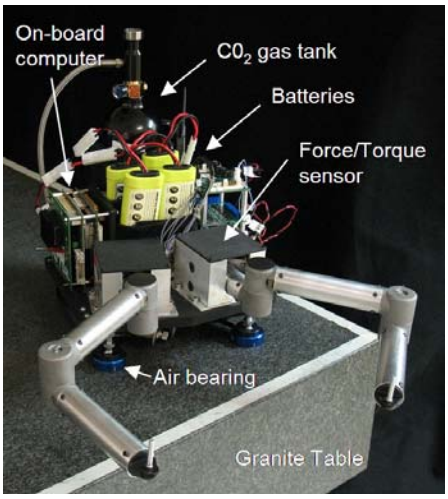

Fig. 9. Experimental space robot.

For the experiments done in this study, the flexible element is a simple aluminum beam, 1.22 m long, 0.80 mm thick. Its lowest natural frequency is 2.8 Hz. It is supported by and pin-jointed to the end effectors of the robots' manipulators. Three accelerometers on the top of the beam are used to measure its vibration.

A. Cases Studied

In the experiments, the robots maneuver a very flexible beam while controlling its vibration. Here the results are presented for two cases: A parallel maneuver case and a rotational maneuver case.

Parallel maneuver: In this case, two robots hold the ends of the beam and moved parallel to each other in the direction of the beam flexibility (the -*X* direction) by 0.5 m, as shown in Fig. 10. The position of both robots was controlled by PD controller. The thrust profile was close to bang-bang control.

Rotational maneuver: In this case, two robots hold both ends of the beam. One robot is commanded to rotate -30 degrees around the second robot, as shown in Fig. 11.

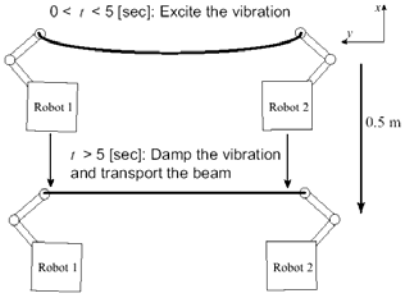

Fig. 10. Case 1: Parallel Maneuver

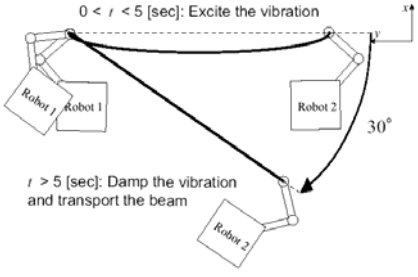

Fig. 11. Case 2: Rotational Maneuver

Fig. 12 shows the timeline used for the experiments. The limited force of the thrusters (~ 0.1 N) prevents the robot's maneuvers alone from exciting visible vibrations. In the experiments the vibrations were excited using the two robot's manipulators for the first 5 seconds of each experiment. The manipulators were given a preprogrammed sinusoidal motion with a frequency of 1.0 Hz for the first 5 seconds. Meanwhile, the robots' position and orientation were maintained by thrusters.

At 5 seconds, experiments were performed using the control methods described above. In the simulation, instead of exciting vibration during the first 5 seconds by manipulators, the initial conditions of first mode vibration were set ($[q_1(0) \quad \dot{q}_1(0)] = [0.2 \quad 0]$). Only the first mode vibration was controlled in this experiment due to the limitations of the controller bandwidth. The action of the thrusters and manipulators for the three control methods are shown in Table I.

For the active vibration control experiments, the parameters in the objective function (Eq. 8 and 9) were set as follows. See Eq. (3) and (4) for the definition of x and u.

$$Q = \begin{bmatrix} 10^4 & 0 & 0 & 0 \\ 0 & 10^4 & 0 & 0 \\ 0 & 0 & 1 & 0 \\ 0 & 0 & 0 & 1 \end{bmatrix} \qquad (11)$$

$$R = \begin{bmatrix} 10^3 & 0 \\ 0 & 10^3 \end{bmatrix} \qquad (12)$$

The attitude control gains were the same for the three control methods.

B. Performance metrics

The performance of the three control methods (shown as (a), (b) and (c) in Table I) were compared using the following two metrics.

Fuel consumption: The total amount of the fuel (CO_2 gas) consumed between t =5 seconds (the start of the vibration control) and the time when the robots were within 3 cm distance (for the parallel maneuver) and 2 degrees (for the rotational maneuver) of their goal positions. The fuel consumption was estimated from the thruster command in the controller log. It did not include the CO_2 gas used to float the robots.

Damping ratio: The damping ratio of the first mode vibration of the beam. The damping ratio captures the ability of the controller to damp out vibration. The time-series vibration amplitude data was obtained from the Kalman filter. The damping ratio was defined as the variable zeta (ζ) in the following vibration equation and was obtained from nonlinear least squares curve fitting:

$$x = A\exp(-\zeta\omega t)\sin(\sqrt{1-\zeta^2}\,\omega t + \phi) \qquad (13)$$

V. Experimental Results

Fig. 13 shows the experimental first mode vibration of the three control methods for a typical parallel maneuver. With the decoupled controller, the vibration was damped in the shortest amount of time. However, a larger disturbance was observed after the vibration was damped with the experimental decoupled control than with no vibration control and thruster vibration control. This is because the manipulator force controller reacted to the sensor noises.

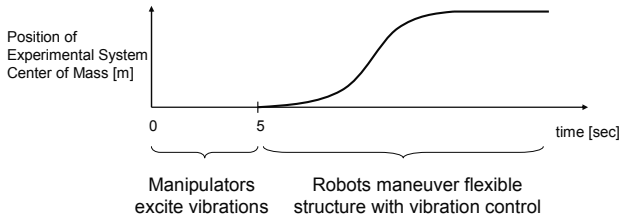

Fig. 12. Experimental timeline.

TABLE I
Experimental Timeline

Control	Components	First 5 Seconds	Remaining Time
(a) No Vibration Control	Thrusters	Control Attitude	Transport beam and control attitude
	Manipulators	Excite Vibration	Locked
(b) Thruster Vibration Control	Thrusters	Control Attitude	Transport beam, control attitude and control vibration
	Manipulators	Excite Vibration	Locked
(c) Maneuver Decoupled Control	Thrusters	Control Attitude	Transport beam and control attitude
	Manipulators	Excite Vibration	Control vibration

Fig. 14 shows experimental results for ten experiments conducted for each of the three control methods for both the parallel and the rotational maneuvers.

The figure compares the damping ratio and fuel consumption of the three control methods. The boxes indicate the average while the bars are standard deviation.

Approximately the same results were obtained for both maneuvers. The damping ratio with decoupled control was about twice of the other two methods. The damping ratio of thruster control was even smaller than no vibration control. This suggests that the thruster vibration controller degraded the system performance.

These results generally agreed with the simulation result shown in Fig. 5, Fig. 6, and Fig. 7, except for two points. The first is that the damping ratio of thruster vibration controller was smaller than no vibration control in the experiment while they were almost the same in the simulation. This implies that the parameters of the experimental hardware used for the simulation model were not well known. A formal identification of the parameters of the experimental system for use in the simulations is future work. The other difference between the experiment and simulation was that decoupled control consumed more fuel than no vibration control in the experiment while the fuel consumption of no vibration control and decoupled control was almost the same in the simulation. In the experiment, the attitude of the robots in decoupled control was not as stable as in the simulation due to the disturbance and actuation error. A substantial amount of fuel was consumed to maintain the attitude of the robots, which made this difference.

VI. Conclusion

This work experimentally validated a large space structure maneuver algorithm, the decoupled controller. The decoupled controller actively controls the vibration of the structure using the space robots' manipulators while using the thrusters for rigid-body motion. The algorithm was shown to double the damping ratio over thruster-based vibration control, while consuming less fuel.

Acknowledgment

Special thanks to Prof. David Miller and the MIT Space Systems Laboratory for the use of their microgravity emulation laboratory.

References

[1] A. K. Banerjee, N. Pedreiro, and W. E. Singhose. Vibration reduction for flexible spacecraft following momentum dumping with/without slewing. AIAA J. of Guidance, Control, and Dynamics, 24(3), 2001.

[2] J. Ben-Asher, J. Burns, and E. Cliff. Time-optimal slewing of flexible spacecraft. AIAA Journal of Guidance, Control and Dynamics, 15(2):360–367, March - April 1992.

[3] H. W. Bennett, C. LaVigna, H. G. Kwatny, G. Blankenship. Nonlinear and adaptive control of flexible space structures. ASME, Transactions, J. of Dyn. Sys., Measurement, and Control, v. 115, March 1993.

[4] H. Bitter, H. Fisher, and M. Surauer. Design of reaction jet attitude control systems for flexible spacecraft. In Proceedings of the Ninth Symposium on Automatic Control in Space, 1982.

[5] Dickson, W.C.; Cannon, R.H., Jr., "Experimental results of two free-flying robots capturing and manipulating a free-flying object", *Proc. of the IEEE Int. Conf. on Intelligent Robots and Systems*, Aug. 1995.

[6] Dunn, H.J., "Experimental Results of Active Control on a Large Structure to Suppress Vibration", *AIAA J. of Guidance, Control and Dynamics*, Vol. 15, No. 6, Nov-Dec. 1992.

[7] Hogan, N., "Impedance Control: An Approach to Manipulation," *ASME J. of Dy. Sys, Meas. and Control*, Vol. 107, March 1985.

[8] Huntsberger, T., Stroupe, A., and Kennedy, B., "System of Systems for Space Construction", *IEEE International Conference on Systems, Man, and Cybernetics*, Waikoloa, Hawaii, October 2005.

[9] Y. Ishijima, D. Tzeranis, and S. Dubowsky. The on-orbit maneuvering of large space flexible structures by free-flying robots. *i-SAIRAS* 2005.

[10] Takashi Kida; Isao Yamaguchi; Yuichi Chida; Takeshi Sekiguchi. Onorbit robust control experiment of flexible spacecraft ets-vi. AIAA Journal of Guidance, Control, and Dynamics, 20(5):865–872, 1997.

[11] Mangalgiri,,V. "Analysis for the Robotic Assembly of Large Flexible Space Structures," MS Thesis, Department of Mech Eng, Massachusetts Institute of Technology, 2004.

[12] Oda, M., Ueno, H., and Mori, M., "Study of the Solar Power Satellite in NASDA", *Proc.7th i-SAIRAS*, Nara, Japan, 2003.

[13] Ono, Masahiro "Experimental Validation of the Efficient Robotic Transportation Algorithm for Large-scale Flexible Space Structures," MS Thesis, Department of Aeronautics and Astronautics, Massachusetts Institute of Technology, 2007.

[14] W. Singhose and H. Okada. Control of flexible satellites using analytic on-off thruster commands. Proc. of the 2003 AIAA Guidance, Navigation, and Control Conf., 2003.

[15] S. D. Smith, M. M. Penny, T. F. Greenwood, and B. B. Roberts. Exhaust plume impingement of chemically reacting gas-particle flows. In *AIAA 10th Thermophysics Conference*, May 1975.

[16] J. Turner and J. Junkins. Optimal large-angle single-axis rotational maneuvers of flexible spacecraft. AIAA Journal of Guidance and Control, 3(6):578 – 585, Nov - Dec 1980.

[17] Whittaker, W., Staritz, P., Ambrose, R., Kennedy, B., Fredrickson, S., Parrish, J., and Urmson, C., "Robotic Assembly of Space Solar-Power Facilities", *Journal of Aerospace Eng.*, Vol. 14, No. 2, April, 2001.

[18] T. Williams. Space station flexible dynamics under plume impingement. Technical Report 2, Johnson Space Center, (NASA)/(ASEE) Summer Faculty Fellowship Program, Dec 1993.

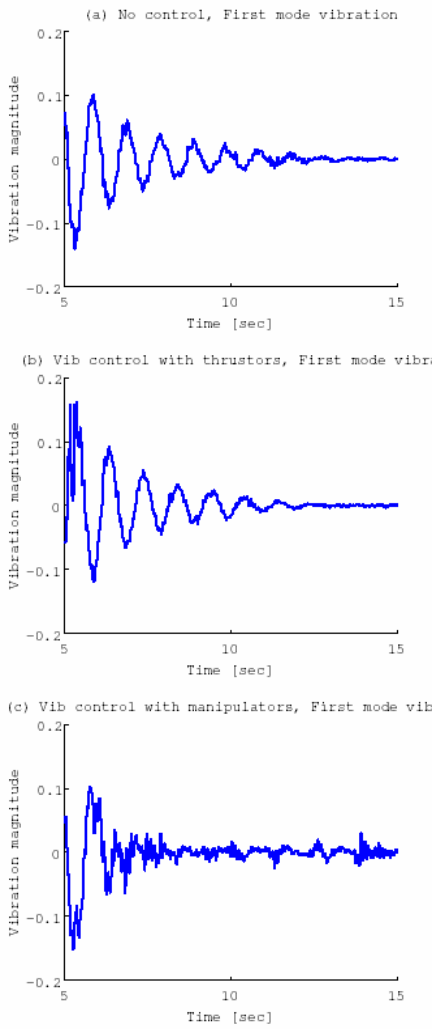

Fig. 13. The first mode vibration of the experiment. (a) No vibration control (b) Thruster vibration control (c) Decoupled control (Vibration control by manipulators)

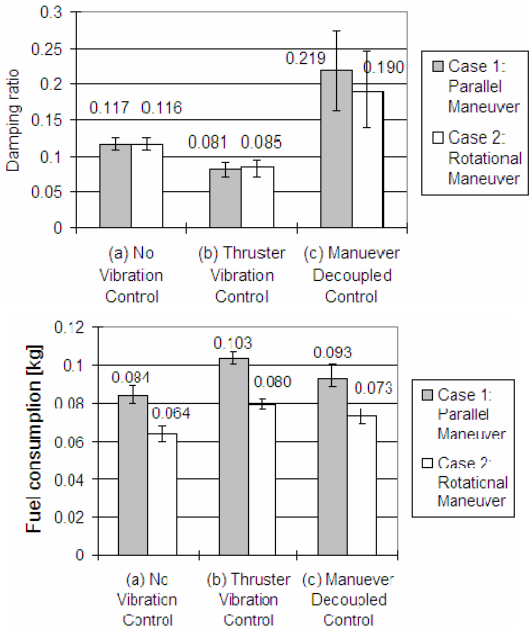

Fig. 14. Damping ratio and fuel consumption of three control methods for parallel and rotational maneuvers (experimental results). Each bar is the result of ten experimental trials.